Hindawi
Complexity
Volume 2022, Article ID 1626008, 13 pages
https://doi.org/10.1155/2022/1626008

WILEY | Hindawi

Research Article

A General Epidemic Model and Its Application to Mask Design Considering Different Preferences towards Masks

Chaoqian Wang and Hamdi Kavak

Department of Computational and Data Sciences, George Mason University, Fairfax 22030, VA, USA

Correspondence should be addressed to Chaoqian Wang; cqwang814921147@outlook.com

Received 24 March 2022; Accepted 28 September 2022; Published 30 October 2022

Academic Editor: Roberto Natella

While most masks have a limited effect on personal protection, how effective are they for collective protection? How to enlighten the design of masks from the perspective of collective dynamics? In this paper, we assume three preferences in the population: (i) never wearing a mask; (ii) wearing a mask if and only if infected; (iii) always wearing a mask. We study the epidemic transmission in an open system within the Susceptible-Infected-Recovered (SIR) model framework. We use agent-based Monte Carlo simulation and mean-field differential equations to investigate the model, respectively. Ternary heat maps show that wearing masks is always beneficial in curbing the spread of the epidemic. Based on the model, we investigate the potential implications of different mask designs from the perspective of collective dynamics. The results show that strengthening the filterability of the mask from the face to the outside is more effective in most parameter spaces because it acts on individuals with both preferences (ii) and (iii). However, when the fraction of individuals always wearing a mask achieves a critical point, strengthening the filterability from outside to the face becomes more effective because of the emerging hidden reality that the infected individuals become too few to utilize the filterability from their face to outside fully.

1. Introduction

As the COVID-19 pandemic is ravaging the world, the protection of masks is a topic of interest. A news article published in Nature indicates that wearing a surgical mask leads to a 11% drop in risk, while a 5% drop for cloth [1]. The protective effect of masks on individuals may seem minimal, but it is also necessary to focus on the protective effect on collectives.

Since Kermack and McKendrick [2] proposed the Susceptible-Infected-Recovered (SIR) compartment model, various epidemic models have been developed considerably. In the classic SIR model, the population is divided into three compartments: (i) the susceptible (S); (ii) the infected (I); (iii) the recovered (R). Through human-to-human contact or self-healing, individuals flow from one compartment to another. A simple modified version is the SEIR model, which adds an exposed (E) compartment to the SIR model. Recently, Barlow et al. [3, 4] derived the analytical solutions of the SIR [3] and the SEIR [4] models.

Researchers, in recent years, have explored additional factors and mechanisms to the classic epidemic models, such as isolation [5] and vaccination [6–11]. The dynamics of the epidemic transmission can also be applied to the information spreading, creating rumor spreading models [12, 13] or the public opinion dynamics model [14, 15]. From the perspective of verification and validation, the global stability of this class of nonlinear dynamical systems is widely studied [16–21]. In particular, researchers have proved the global stability of endemic equilibria in various epidemic models in multigroup populations [19–21], which are general cases of the model proposed in this work. A common approach to prove global stability is constructing a Lyapunov function (not limited to epidemiology but also widely applied to other complex systems such as evolutionary dynamics [22, 23]), which measures the system's "energy." If the energy

continues to decay, then the system will stabilize at an equilibrium point.

When it comes to the protective effect of masks, several works [24–28] are noticed to have emerged in the COVID-19 period after 2020. Li et al. [24] treated whether people wear masks or not as an evolutionary game. Gondim [25] considered masks in the SEIR model and validated the model by real-world data. Auger and Moussaoui [26] studied the confinement's release threshold, taking the masks into account. Lasisi and Adeyemo [27] modeled the effect of wearing masks on COVID-19 infection dynamics. Han et al. [28] investigated the effect of three different preferences on wearing a mask.

Based on the existing literature, we find the previous works on masks have three shortcomings. First, when classifying the population into three categories with different preferences on wearing masks according to their assumptions, there is no work classifying them into three independent variables. They set only two variables as the fraction of two categories, and the remaining category's fraction is one minus these two variables. This leads to an inability to ensure constant relative proportions of the other two categories when investigating the effect of the proportion of a certain category. Second, previous work did not carry out a complete analysis of the stability of their models. This makes verification and validation challenging. Third, only focusing on the effect of masks on epidemic spreading, there is no previous work considering providing applications of the epidemic models to the design of masks itself.

This paper builds a general epidemic model in an open system considering three different preferences on wearing masks. We start from a set of agent-based rules, and use mean-field analysis to verify and validate the model. In addition to filling in the gaps of previous work by treating three preferences as independent variables and considering global stability analysis, we explore [29, 30] the effect of different preferences towards wearing masks on the epidemic transmission through our model's eyes. Considering that in the traditional perception, masks are designed at an individual level, we also try to reveal the design strategies of the masks by the collective dynamics based on our model.

2. Model

There is an epidemic disease spreading in the system. To prevent this epidemic, individuals hold different preferences for wearing masks. Concerning the infection state, we divide the population into (i) the susceptible (x); (ii) the infected (y); (iii) the recovered (z). In terms of different preferences towards wearing masks, we divide the population into (i) those who never wear masks (subscript 0); (ii) those who wear masks if and only if infected (subscript 1); (iii) those who always wear masks (subscript 2). Therefore, we have up to 9 categories according to different combinations of the classification of the two dimensions mentioned above.

Before describing evolutionary rules, we list the definition of our mathematical symbols in Table 1.

2.1. The Agent-Based Rules. Consider an open system containing initially $n|_{t=0}$ agents (i.e., individuals). Within a Monte Carlo step, an agent i is randomly selected, and the following parallel events occur.

(1) If agent i is susceptible, we again select an agent j randomly. If agent j is infected, then agent i is infected with a probability $\alpha\,(\alpha > 0)$. If agent j wears a mask, then agent i spares from infection with a probability $p_I\,(0 < p_I < 1)$. If agent i wears a mask, then agent i spares from infection with a probability $p_S\,(0 < p_S < 1)$.

(2) If agent i is infected, then it recovers with a probability r (the average infection cycle is $1/r$). This does not happen at the same Monte Carlo step as the event (1).

(3) Agent i naturally dies with a probability μ (the average lifespan is $1/\mu$). We do not consider deaths due to the epidemic.

To ensure the population remains almost unchanged, we must let new agents enter the system. We set the following very first event in a Monte Carlo step, where the number (0) means it happens before the event (1).

(0) A new agent enters the system with a probability p_e. The agent's personal preference determines it never wears a mask with a probability $\varepsilon_0\,(0 < \varepsilon_0 < 1)$, wears a mask if and only if infected with a probability $\varepsilon_1\,(0 < \varepsilon_1 < 1)$, or always wears a mask with a probability $\varepsilon_2\,(0 < \varepsilon_2 < 1)$, yielding $\varepsilon_0 + \varepsilon_1 + \varepsilon_2 = 1$. The preference of an agent on masks does not change over time.

For the population n remaining almost unchanged with time, we let one time step t contains $n|_{t=0}$ Monte Carlo steps, such that each agent can be selected once on average. Therefore, the expected number of new agents entering the system within one time step t is $\Lambda = n^* p_e$. The solution is $p_e = \mu$ (see Theorem 1).

2.2. The Mean-Field Equations. Performing mean-field analysis, we can approximate the agent-based dynamics into a set of differential equations. We do not dwell on the principles of mean-field analysis, but only explain some important points. (i) Within unit time, each agent is selected once on average, such that the number of events descending in a category is the population in the category. (ii) The probability of selecting an infected agent never wearing a mask from the population is y_0/n, and y_1/n, y_2/n for selecting an infected agent holding the other two preferences, respectively. (iii) Thanks to the mask, the probability of sparing from infection is p_I or p_S, which means the probability of infection is $(1 - p_I)$ or $(1 - p_S)$. (iv) If there are two layers of protection, they must be both breached for the infection to succeed.

We denote the state of the system by a vector ψ, containing the population in nine categories. The mean-field differential equations depicting the agent-based dynamics is

$$\dot{\Psi} = \begin{pmatrix} \dot{x}_0 \\ \dot{y}_0 \\ \dot{z}_0 \\ \dot{x}_1 \\ \dot{y}_1 \\ \dot{z}_1 \\ \dot{x}_2 \\ \dot{y}_2 \\ \dot{z}_2 \end{pmatrix}, \tag{1}$$

where

$$\begin{cases} \dot{x}_0 = \varepsilon_0\Lambda - \alpha x_0 \dfrac{[y_0 + (1-p_I)(y_1+y_2)]}{n - \mu x_0}, \\ \dot{y}_0 = \alpha x_0 \dfrac{[y_0 + (1-p_I)(y_1+y_2)]}{n - ry_0 - \mu y_0}, \\ \dot{z}_0 = ry_0 - \mu z_0, \\ \dot{x}_1 = \varepsilon_1\Lambda - \alpha x_1 \dfrac{[y_0 + (1-p_I)(y_1+y_2)]}{n - \mu x_1}, \\ \dot{y}_1 = \alpha x_1 \dfrac{[y_0 + (1-p_I)(y_1+y_2)]}{n - ry_1 - \mu y_1}, \\ \dot{z}_1 = ry_1 - \mu z_1, \\ \dot{x}_2 = \varepsilon_2\Lambda - \alpha(1-p_S) x_2 \dfrac{[y_0 + (1-p_I)(y_1+y_2)]}{n - \mu x_2}, \\ \dot{y}_2 = \alpha(1-p_S) x_2 \dfrac{[y_0 + (1-p_I)(y_1+y_2)]}{n - ry_2 - \mu y_2}, \\ \dot{z}_2 = ry_2 - \mu z_2. \end{cases} \tag{2}$$

The system depicted by (1) is an extended version of the SIR model with a standard incidence rate.

3. Results and Discussion

In this section, we demonstrate the numerical results of the model from both Monte Carlo simulation and mean-field equations. The algorithm of the Monte Carlo simulation was described in Section 2.1. In the numerical simulation of mean-field equations, we use iteration $\Psi(t + \Delta t) = \Psi(t) + \dot{\Psi}(t)\Delta t$, where $\Delta t = 0.01$.

We set three statistical measures: (i) the proportion of susceptible, $p_x = (x_0 + x_1 + x_2)/n$; (ii) the proportion of infected, $p_y = (y_0 + y_1 + y_2)/n$; (iii) the proportion of recovered, $p_z = (z_0 + z_1 + z_2)/n$.

3.1. Impact of Masks on Epidemic Spreading. Figures 1 and 2 show the time evolution of p_x, p_y, and p_z with different parameters and initial conditions.

From Figures 1 and 2, we find the proportions of different individuals always achieve stability after time evolution. The results of the Monte Carlo simulation fluctuate, while the results of mean-field equations are stable. They corroborate each other. In addition, we obverse two phenomena. First, the epidemic may either die out or exist at the end, dependent on different parameters. Second, with the same parameters and different initial conditions, the steady-states are the same.

Next, in the heat maps Figures 3 and 4, we present the steady-states of p_y and p_x as a ternary function of ε_0, ε_1, ε_2, respectively. The results of the Monte Carlo simulation are the average of the last 200 time steps (t). The results of mean-field equations are retrieved from the state $\Psi(t + \Delta t)$ when $\max\{|\Psi(t)|\Delta t\} < 0.0001$.

From Figures 3 and 4, we find that the results of Monte Carlo simulation and mean-field equations corroborate each other. In Figure 3, we observe that more individuals wearing masks reduce the proportion of infected individuals in the population. In particular, always wearing a mask has a better effect on reducing infected individuals. In Figure 4, we observe that more individuals wearing masks increases the proportion of susceptible individuals in the population. Different from increasing recovered individuals, it means that more people are spared from getting infected once. Also, always wearing a mask has a better effect on increasing susceptible individuals (Figure 4), making more individuals spared from being infected.

3.2. Potential Implication of Different Mask Designs. Based on our model, we can reveal the potential implication of different mask designs. When an infected individual wears a mask, it is the filterability from the face to the outside that provides protection (to the population), and when a susceptible individual wears a mask, the filterability from the outside to the face matters.

We show in Figures 5(a) and 5(b) the steady infected fraction p_y as a binary function of the protective effect produced when an infected individual wears a mask (p_I) and when a susceptible individual wears a mask (p_S).

We can observe that in both the Monte Carlo simulation (Figure 5(a)) and mean-field equations (Figure 5(b)), an increase in protective effect p_I or p_S leads to a decrease in the steady infected fraction p_y. On this basis, we further ask which one in increasing p_I or p_S is more effective in reducing the infected fraction?

We show in Figure 5(c) the steady-state of $\partial p_y/\partial p_I$ and $\partial p_y/\partial p_S$ as a binary function of p_I and p_S. If $\partial p_y/\partial p_I < \partial p_y/\partial p_S$, increasing the unit protective effect from the infected side is more conducive to reducing the infected fraction, and vice versa. Intuitively, increasing p_I should have always been more conducive than increasing p_S because the former acts on individuals with two preferences, (ii) those who wear masks if and only if infected and (iii) those who always wear masks. In contrast, the latter only acts

Table 1: The definition of mathematical symbols.

Symbol	Definition
x_0	The number of susceptible individuals never wearing a mask.
y_0	The number of infected individuals never wearing a mask.
z_0	The number of recovered individuals never wearing a mask.
x_1	The number of susceptible individuals wearing a mask if and only if infected.
y_1	The number of infected individuals wearing a mask if and only if infected.
z_1	The number of recovered individuals wearing a mask if and only if infected.
x_2	The number of susceptible individuals always wearing a mask.
y_2	The number of infected individuals always wearing a mask.
z_2	The number of recovered individuals always wearing a mask.
n	The number of individuals in the system.
Λ	The number of new individuals entering the system within unit time.
μ	The rate of natural death.
r	The rate of recovering.
α	The rate of human-to-human infection.
ε_0	The fraction of new individuals never wearing a mask.
ε_1	The fraction of new individuals wearing a mask if and only if infected.
ε_2	The fraction of new individuals always wearing a mask.
p_I	The protective effect produced when an infected individual wears a mask.
p_S	The protective effect produced when a susceptible individual wears a mask.

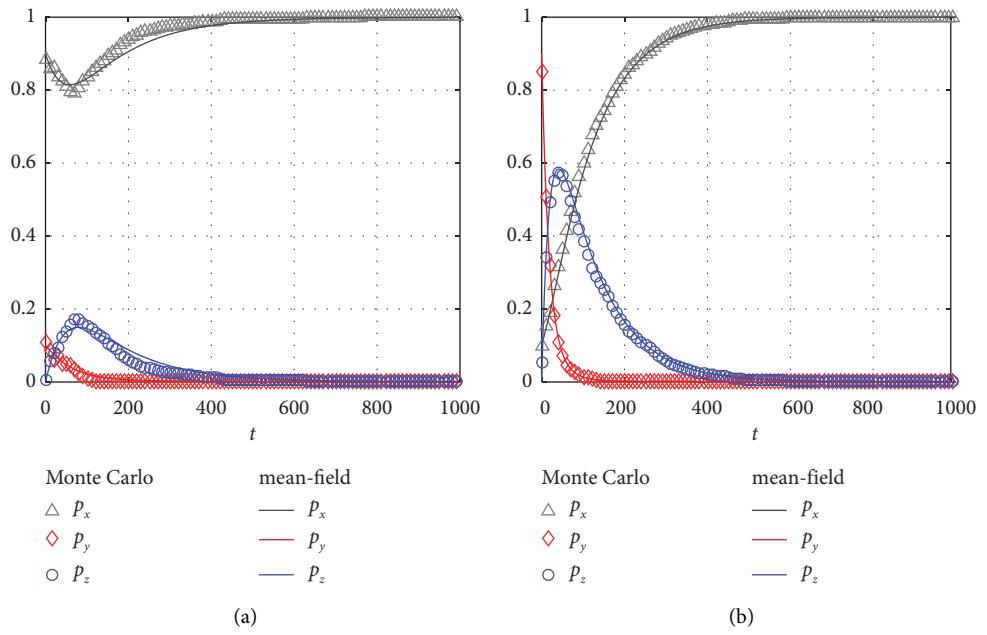

Figure 1: Time evolution of p_x, p_y, and p_z. The results of Monte Carlo simulation and mean-field equations are presented together. $\alpha = 0.2$, $\mu = 0.01$, $\Lambda = 10$, $r = 0.05$, $\varepsilon_0 = 0.1$, $\varepsilon_1 = 0.1$, $\varepsilon_2 = 0.8$, $p_I = 0.75$, $p_S = 0.25$. (a) $p_x|_{t=0} = 0.9$, $p_y|_{t=0} = 0.1$, $p_z|_{t=0} = 0$. (b) $p_x|_{t=0} = 0.1$, $p_y|_{t=0} = 0.9$, $p_z|_{t=0} = 0$. (a) (b) $x_0|_{t=0} = x_1|_{t=0} = x_2|_{t=0}$ in $x|_{t=0}$, as well as $y|_{t=0}$ and $z|_{t=0}$.

on individuals with one preference, (iii) those who always wear masks. Increasing p_I obviously has a broader scope of action than the increasing p_S and covers the latter's population. However, Figure 5(c) presents a different phenomenon. This indicates that we can provide the designs of the masks with different insights from the group dynamics. We will give this further analysis in Section 4.5.

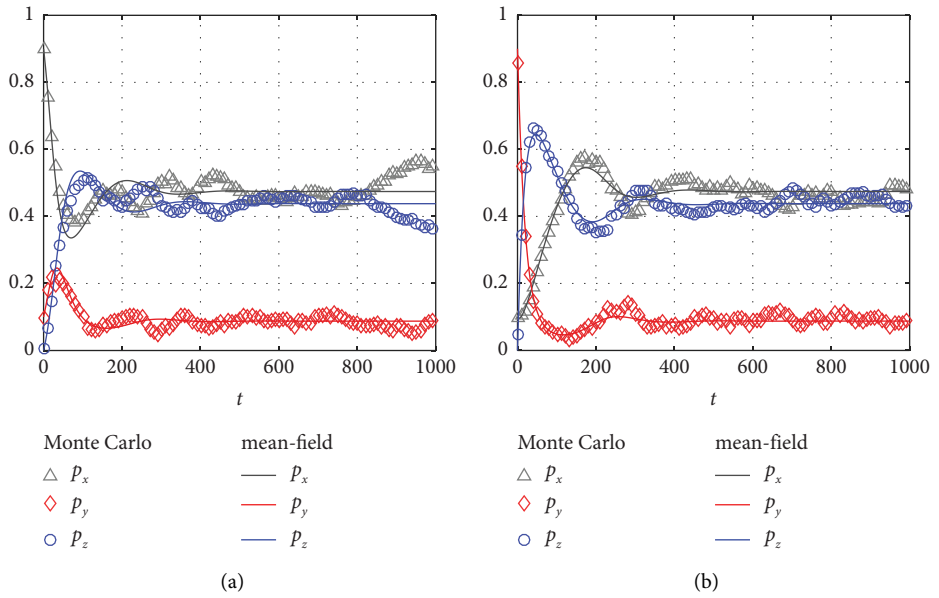

Figure 2: Time evolution of p_x, p_y, and p_z. The results of Monte Carlo simulation and mean-field equations are presented together. $\alpha = 0.2$, $\mu = 0.01$, $\Lambda = 10$, $r = 0.05$, $\varepsilon_0 = 0.3$, $\varepsilon_1 = 0.1$, $\varepsilon_2 = 0.6$, $p_I = 0.5$, $p_S = 0.05$. (a) $p_x|_{t=0} = 0.9$, $p_y|_{t=0} = 0.1$, $p_z|_{t=0} = 0$. (b) $p_x|_{t=0} = 0.1$, $p_y|_{t=0} = 0.9$, $p_z|_{t=0} = 0$. (a) (b) $x_0|_{t=0} = x_1|_{t=0} = x_2|_{t=0}$ in $x|_{t=0}$, as well as $y|_{t=0}$ and $z|_{t=0}$.

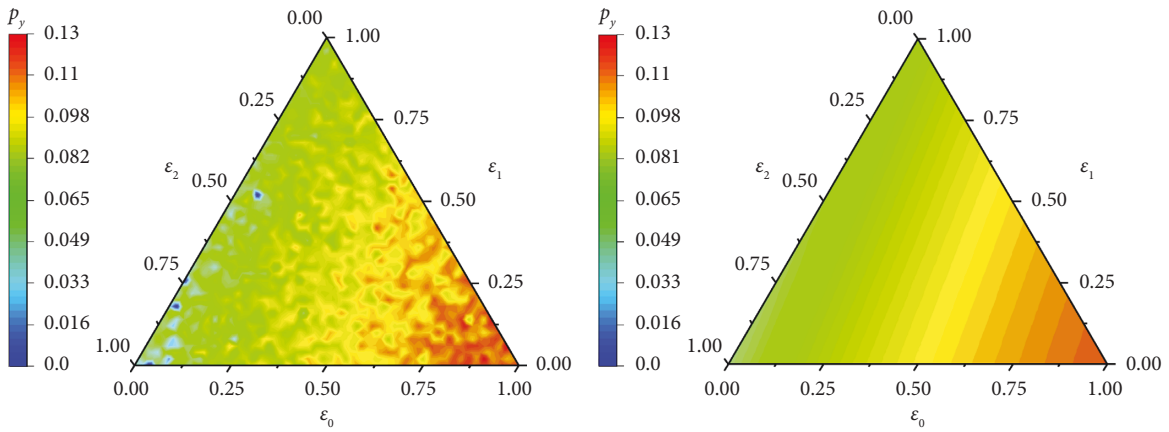

Figure 3: The steady-state of p_y as a ternary function of ε_0, ε_1, ε_2. (a) Monte Carlo simulation. (b) Mean-field equations. $\alpha = 0.2$, $\mu = 0.01$, $\Lambda = 10$, $r = 0.05$, $p_I = 0.5$, $p_S = 0.05$.

4. Verification and Validation

This section verifies and validates the properties that we concluded in numerical results by analyzing them at a mathematical level.

4.1. The Total Population Dynamics. The total population dynamics follows Theorem 1.

Theorem 1. *For $t \longrightarrow \infty$, we have $n \longrightarrow \Lambda/\mu$.*

Proof. According to (1),

$$\dot{n} = \dot{x}_0 + \dot{y}_0 + \dot{z}_0 + \dot{x}_1 + \dot{y}_1 + \dot{z}_1 + \dot{x}_2 + \dot{y}_2 + \dot{z}_2 = \Lambda - \mu n. \tag{3}$$

Solving (3), we get

$$n = \left(n|_{t=0} - \frac{\Lambda}{\mu}\right)e^{-\mu t} + \frac{\Lambda}{\mu}. \tag{4}$$

From (4), we complete the proof that $n \longrightarrow \Lambda/\mu$ for $t \longrightarrow \infty$. We give this significant value a symbol n^*,

$$n^* = \lim_{t \longrightarrow \infty} n = \frac{\Lambda}{\mu}. \tag{5}$$

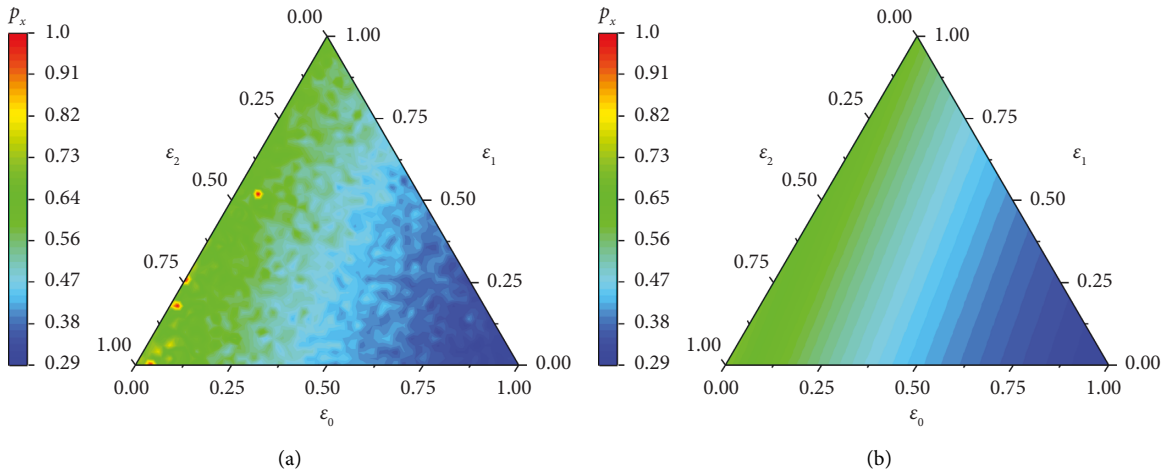

FIGURE 4: The steady-state of p_x as a ternary function of ε_0, ε_1, ε_2. (a) Monte Carlo simulation. (b) Mean-field equations. $\alpha = 0.2$, $\mu = 0.01$, $\Lambda = 10$, $r = 0.05$, $p_I = 0.5$, $p_S = 0.05$.

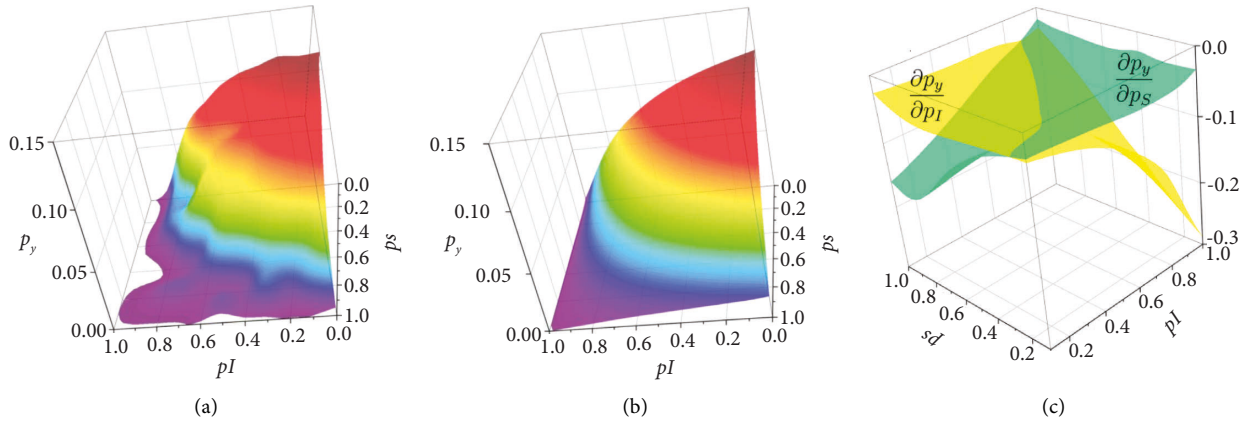

FIGURE 5: (a) Monte Carlo simulation. The steady-state of p_y as a binary function of p_I, p_S. (b) Mean-field equations. The steady-state of p_y as a binary function of p_I, p_S. (c) Mean-field equations. The steady-state of $\partial p_y/\partial p_I$ and $\partial p_y/\partial p_S$ as a binary function of p_I, p_S. $\alpha = 0.2$, $\mu = 0.01$, $\Lambda = 10$, $r = 0.05$, $\varepsilon_0 = 0.3$, $\varepsilon_1 = 0.1$, $\varepsilon_2 = 0.6$, $p_I = 0.5$, $p_S = 0.05$.

In the same way, we can also prove that $x_0 + y_0 + z_0 \longrightarrow \varepsilon_0\Lambda/\mu$, $x_1 + y_1 + z_1 \longrightarrow \varepsilon_1\Lambda/\mu$, $x_2 + y_2 + z_2 \longrightarrow \varepsilon_2\Lambda/\mu$ for $t \longrightarrow \infty$.

Theorem 1 gives us another important insight: when discussing the steady-state, we can substitute n for $n^* = \Lambda/\mu$ in the system of (1). □

4.2. The Basic Reproduction Number. The basic reproduction number $\mathcal{R}_0$ is one of the most important measures in epidemiology. It can assist in analyzing both the stability of the system and the effect of parameters on the epidemic transmission.

We let $\dot{\Psi} = 0$ and solve for the epidemic-free equilibrium, denoted by Ψ^*,

$$\Psi^* = \frac{\Lambda}{\mu}(\varepsilon_0, 0, 0, \varepsilon_1, 0, 0, \varepsilon_2, 0, 0)^T. \tag{6}$$

Then, we can follow the meWthod in [31] to find the basic reproduction number (see Appendix A):

$$\mathcal{R}_0 = \frac{\alpha}{r+\mu}\left[\varepsilon_0 + (1-p_I)\varepsilon_1 + (1-p_S)(1-p_I)\varepsilon_2\right]. \tag{7}$$

The basic reproduction number reveals the following theorem.

Theorem 2. *The epidemic-free equilibrium Ψ^* is locally asymptotically stable if $\mathcal{R}_0 < 1$, and the epidemic-free equilibrium Ψ^* is not stable if $\mathcal{R}_0 > 1$.*

(See [31] for proof).

Substituting the parameters in Figure 1 into Equation (A.5), we can calculate $\mathcal{R}_0 = 0.9167 < 1$, which means the epidemic-free equilibrium is stable, consistent with that shown in Figure 1. Similarly, substituting parameters in Figure 2 produces $\mathcal{R}_0 = 2.1167 > 1$, such that the epidemic-

free equilibrium is not stable, which is also consistent with that shown in Figure 2.

4.3. Epidemic-Free and Endemic Equilibria. We separate Ψ into

$$\begin{cases} \mathbf{\Phi}_1 = (x_0, y_0, x_1, y_1, x_2, y_2)^{\mathrm{T}}, \\ \mathbf{\Phi}_2 = (z_0, z_1, z_2)^{\mathrm{T}}. \end{cases} \tag{8}$$

From (1), we can assert that the steady-state of $\mathbf{\Phi}_1$ can determine the steady-state of $\mathbf{\Phi}_2$, and $\mathbf{\Phi}_2$ does not affect the evolution of $\mathbf{\Phi}_1$. Therefore, the stability of Ψ is equivalent to (i) the stability of $\mathbf{\Phi}_1$ and (ii) the stability of $\mathbf{\Phi}_2$ when $\mathbf{\Phi}_1$ achieves stability.

We first prove the global stability of the epidemic-free equilibrium by constructing the Lyapunov function.

Theorem 3. *The epidemic-free equilibrium Ψ^* is global asymptotically stable in $\mathbb{R}^9_{\geq 0}$ if $\mathscr{R}_0 < 1$.*

Proof. Consider the Lyapunov function $\mathscr{L}(\mathbf{\Phi}_1)$ in $\mathbb{R}^6_{\geq 0}$,

$$\mathscr{L}(\mathbf{\Phi}_1) = \frac{(x_0 - x_0^*)^2}{2x_0^*} + y_0 + (1 - p_I)\left[\frac{(x_1 - x_1^*)^2}{2x_1^*} + y_1\right] + (1 - p_I)\left[\frac{(x_2 - x_2^*)^2}{2x_2^*} + y_2\right]. \tag{9}$$

We can conclude that, (i) $\mathscr{L}(\mathbf{\Phi}_1) = 0$ when $\mathbf{\Phi}_1 = \mathbf{\Phi}_1^*$, (ii) $\mathscr{L}(\mathbf{\Phi}_1) > 0$ when $\mathbf{\Phi}_1 \neq \mathbf{\Phi}_1^*$. Therefore, $\mathbf{\Phi}_1$ is positive definite in the neighborhood of $\mathbf{\Phi}_1^*$. Secondly, we have (see Appendix B),

$$\dot{\mathscr{L}}(\mathbf{\Phi}_1) \leq 0, \tag{10}$$

when $\mathbf{\Phi}_1 \neq \mathbf{\Phi}_1^*$. Note that $\dot{\mathscr{L}}(\mathbf{\Phi}_1) = 0$ can be confirmed by Equation (B.1) when $\mathbf{\Phi}_1 = \mathbf{\Phi}_1^*$. Therefore, $\mathbf{\Phi}_1$ is negative semidefinite in the neighborhood of $\mathbf{\Phi}_1^*$. Hence, according to Lasalle's Invariance Principle [32], $\mathbf{\Phi}_1^*$ is globally asymptotically stable in $\mathbb{R}^6_{\geq 0}$. Given $\mathbf{\Phi}_1^*$ stable, it is easy to prove the global asymptotic stability of $\mathbf{\Phi}_2^*$ in $\mathbb{R}^3_{\geq 0}$ by constructing Lyapunov function $\mathscr{L}_z(\mathbf{\Phi}_2) = z_0 + z_1 + z_2$. Therefore, Ψ^* is global asymptotically stable in $\mathbb{R}^9_{\geq 0}$.

The equation $\dot{\Psi} = 0$ has two solutions. We denote the second solution by Ψ^{**}. The infected population is nonzero; thus, we call it the endemic equilibrium. This equilibrium Ψ^{**} corresponds to the results shown in Figure 2. It is not easy to express it analytically, but we can still show its existence condition. □

Theorem 4. *The endemic equilibrium Ψ^{**} exists and is unique in $\mathbb{R}^9_{\geq 0}$ if $\mathscr{R}_0 > 1$.*

Proof. First, we show the relationship between the existence and uniqueness of positive y_i^{**}, $i = 0, 1, 2$ ($y_0^{**} > 0$, $y_1^{**} > 0$, $y_2^{**} > 0$) and $\mathscr{R}_0 > 1$ (see Appendix C). Then, the existence and uniqueness of x_i^{**}, z_i^{**}, $i = 0, 1, 2$ can be naturally confirmed, hence the existence and uniqueness of Ψ^{**}.

Theorem 3 validates that in Figure 1, the steady-state with the same parameters is independent of the initial conditions. Theorem 4 is consistent with Figure 2. □

4.4. Robustness Analysis for the Effect of Wearing Masks. The basic reproduction number measures the average number of individuals that an infected individual can transmit the epidemic. The higher the basic reproduction number, the more severe the epidemic.

Analyzing Equation (A.5), we can see that the coefficient before ε_0 is 1, and $(1 - p_I)$ for ε_1, and $(1 - p_S)(1 - p_I)$ for ε_2. Since $p_S > 0$, $p_I > 0$, we have $(1 - p_S)(1 - p_I) < 1 - p_I < 1$. Considering the constraints: $0 \leq \varepsilon_0 \leq 1$, $0 \leq \varepsilon_1 \leq 1$, $0 \leq \varepsilon_2 \leq 1$, $\varepsilon_0 + \varepsilon_1 + \varepsilon_2 = 1$, we know the following facts. (i) $\mathscr{R}_0$ takes the minimum when $\varepsilon_0 = 0$, $\varepsilon_1 = 0$, $\varepsilon_2 = 1$. (ii) $\mathscr{R}_0$ takes the maximum when $\varepsilon_0 = 1$, $\varepsilon_1 = 0$, $\varepsilon_2 = 0$. Therefore, everyone always wearing a mask minimizes the epidemic severity, while no one wearing masks maximizes the epidemic severity.

4.5. Application to Mask Design. The basic reproduction number $\mathscr{R}_0$ can play the same role as the infected fraction p_y in measuring the outbreak severity. From Equation (A.5), we see that the coefficient $(1 - p_I)$ acts on both ε_1 and ε_2 while $(1 - p_S)$ only acts on ε_2, which means the mask protection from the infected side acts on two population categories and that from the susceptible side acts on only one. This brings us a misleading intuition that increasing the protective effect from the infected side is always more conducive. However, we can reveal a hidden different reality by group dynamics.

We write the partial derivatives of $\mathscr{R}_0$ with respect to p_I and p_S in (11) and (12).

$$\frac{\partial \mathscr{R}_0}{\partial p_I} = -\frac{\alpha}{r + \mu}[\varepsilon_1 + (1 - p_S)\varepsilon_2], \tag{11}$$

$$\frac{\partial \mathscr{R}_0}{\partial p_S} = -\frac{\alpha}{r + \mu}(1 - p_I)\varepsilon_2. \tag{12}$$

Increasing the protective effect from the infected side is better than that of the susceptible one means

$$\frac{\partial \mathscr{R}_0}{\partial p_I} < \frac{\partial \mathscr{R}_0}{\partial p_S}, \tag{13}$$

or

$$\frac{\varepsilon_1}{\varepsilon_2} > p_S - p_I, \tag{14}$$

and increasing the protective effect from the susceptible side is better than that of the infected one means

$$\frac{\partial \mathscr{R}_0}{\partial p_S} < \frac{\partial \mathscr{R}_0}{\partial p_I}, \tag{15}$$

or

$$\frac{\varepsilon_1}{\varepsilon_2} < p_S - p_I. \tag{16}$$

We can discuss the parameter space in two cases. First, if $p_S < p_I$, then (13) always holds. Second, if $p_S > p_I$, then (15) does not always hold. This suggests that the "intuitive" phenomena (increasing p_I is more effective) occupy more parameter space, which can be verified by Figure 5(c).

For the latter case, $p_S > p_I$, we can transform (16) into $\varepsilon_2 > \varepsilon_1/(p_S - p_I)$. This indicates that if the fraction of individuals always wearing a mask (ε_2) exceeds a critical point, $\varepsilon_1/(p_S - p_I)$, then, increasing p_S is more effective than increasing p_I, even if p_I can act on both category ε_1 and ε_2. We can interpret this result in daily language by taking into account the fraction of existing infected individuals. As we showed in Section 4.4, $\mathscr{R}_0$ decreases (i.e., infected individuals increasing) with an increase in ε_2. In this way, the critical point of ε_2 is rational to exist, over which the infected individuals are too few to exert the protective effect that the mask produces on their side.

5. Conclusion

Although most masks have little to no effect on personal protection [1], we are still interested in the protective effects of masks on a population. We proposed a general epidemic model in the classic SIR framework considering three different preferences towards wearing masks. Some individuals never wear masks; others wear masks if and only if infected, and some always wear masks. We started from agent-based rules and used a set of mean-field differential equations to approximate the model. The results of the two corroborate each other. In this work, the three preferences are independent of each other.

The first aspect is the effect of masks on epidemics. The ternary heat maps revealed that wearing masks can reduce the number of infected individuals and increase the number of susceptible individuals. We provided the global stability analysis of the results and showed the robustness of the effectiveness of masks by analyzing the basic reproduction number of the epidemic. We concluded that wearing masks are beneficial to the control of epidemics.

The second aspect is the application of the epidemic model to mask design. The protective effect from the infected side (p_I) can be understood as the filterability of the mask from the face to the outside against viruses, while the protective effect to the susceptible side (p_S) can be interpreted as the filterability from the outside to the face. This can be influenced by the material and design of the mask [33], and we analyzed which side strengthening would provide better results. We showed that strengthening the infected side is more effective in most parameter spaces. This is intuitive since strengthening the infected side acts on two categories of individuals (those wearing masks only if infected and those always wearing masks), while strengthening the susceptible side acts on only one category (those always wearing masks). However, there is a hidden reality from the perspective of group dynamics. We found that once the fraction of individuals always wearing masks exceeds a critical point, $\varepsilon_2 > \varepsilon_1/(p_S - p_I)$, then, strengthening the susceptible side becomes more effective. This is because the preference of always wearing masks reduces the infected fraction in the population, so that the infected individuals are too few to exert the protective effect of masks produced on their side. In the daily language, both the cases above seem to make sense. However, noticing the latter case from the group perspective and further giving the mask design strategies according to parameter spaces are not straightforward without the help of system dynamics.

Real-world situations may have more complexity and different insights. For instance, the underlying assumptions—people's preferences do not change with time, ignores human subjectivity, which has the potential to reveal more insights. In fact, people can change their preference on whether to wear masks by either estimating the epidemic severity (evolutionary games) or being affected by the propaganda of the effectiveness of masks (opinion dynamics). In this way, future work may consider time-dependent preferences, and apply any modified model to mask design.

Appendix

A. Finding the Basic Reproduction Number

Let us decompose the infected compartments in Equation (1) as $(\dot{y}_0, \dot{y}_1, \dot{y}_2)^{\mathrm{T}} = \mathscr{F} - \mathscr{V}$, where

$$\mathscr{F} = \begin{pmatrix} \mathscr{F}_{y_0} \\ \mathscr{F}_{y_1} \\ \mathscr{F}_{y_0} \end{pmatrix} = \begin{pmatrix} \alpha x_0 \dfrac{[y_0 + (1-p_I)(y_1+y_2)]}{n^*} \\ \alpha x_1 \dfrac{[y_0 + (1-p_I)(y_1+y_2)]}{n^*} \\ \alpha(1-p_S)x_2 \dfrac{[y_0 + (1-p_I)(y_1+y_2)]}{n^*} \end{pmatrix}, \tag{A.1}$$

$$\mathscr{V} = \begin{pmatrix} \mathscr{V}_{y_0} \\ \mathscr{V}_{y_1} \\ \mathscr{V}_{y_0} \end{pmatrix} = \begin{pmatrix} ry_0 + \mu y_0 \\ ry_1 + \mu y_1 \\ ry_2 + \mu y_2 \end{pmatrix}. \tag{A.2}$$

Solve for the Jacobian matrix of $\mathscr{F}$ and $\mathscr{V}$ at Ψ^*, denoted by $\mathbf{F}$ and $\mathbf{V}$,

$$\mathbf{F}$$

$$(\boldsymbol{\Psi}^*) = \frac{1}{n^*}\begin{pmatrix} \alpha x_0 & \alpha(1-p_I)x_0 & \alpha(1-p_I)x_0 \\ \alpha x_1 & \alpha(1-p_I)x_1 & \alpha(1-p_I)x_1 \\ \alpha(1-p_S)x_2 & \alpha(1-p_S)(1-p_I)x_2 & \alpha(1-p_S)(1-p_I)x_2 \end{pmatrix} \tag{A.3}$$

$$= \alpha\begin{pmatrix} x_0 & (1-p_I)x_0 & (1-p_I)x_0 \\ x_1 & (1-p_I)x_1 & (1-p_I)x_1 \\ (1-p_S)x_2 & (1-p_S)(1-p_I)x_2 & (1-p_S)(1-p_I)x_2 \end{pmatrix},$$

$$\mathbf{V}$$

$$(\boldsymbol{\Psi}^*) = (r+\mu)\begin{pmatrix} 1 & 0 & 0 \\ 0 & 1 & 0 \\ 0 & 0 & 1 \end{pmatrix}. \tag{A.4}$$

Then, the spectral radius (i.e., maximum eigenvalue) of $\mathbf{F}\cdot\mathbf{V}^{-1}$ is the basic reproduction number $\mathscr{R}_0$,

$$\mathscr{R}_0 = \frac{\alpha}{r+\mu}\left[\varepsilon_0 + (1-p_I)\varepsilon_1 + (1-p_S)(1-p_I)\varepsilon_2\right]. \tag{A.5}$$

Please see [31] for more information on how to find the basic reproduction number.

B. Proof of $\dot{\mathscr{L}}(\boldsymbol{\Phi}_1) \le 0$ When $\boldsymbol{\Phi}_1 \neq \boldsymbol{\Phi}_1^*$

$$\begin{aligned}
&\dot{\mathscr{L}}(\boldsymbol{\Phi}_1) \\
&= \left(\frac{x_0}{x_0^*} - 1\right)\left(\varepsilon_0\Lambda - \frac{\alpha x_0[y_0 + (1-p_I)(y_1+y_2)]}{n^*} - \mu x_0\right) + \frac{\alpha x_0[y_0 + (1-p_I)(y_1+y_2)]}{n^*} \\
&\quad - ry_0 - \mu y_0 + (1-p_I)\left(\frac{x_1}{x_1^*} - 1\right)\left(\varepsilon_1\Lambda - \frac{\alpha x_1[y_0 + (1-p_I)(y_1+y_2)]}{n^*} - \mu x_1\right) \\
&\quad + (1-p_I)\left(\frac{\alpha x_1[y_0 + (1-p_I)(y_1+y_2)]}{n^*} - ry_1 - \mu y_1\right) \\
&\quad + (1-p_I)\left(\frac{x_2}{x_2^*} - 1\right)\left(\varepsilon_2\Lambda - \frac{\alpha(1-p_S)x_2[y_0 + (1-p_I)(y_1+y_2)]}{n^*} - \mu x_2\right) \\
&\quad + (1-p_I)\left(\frac{\alpha(1-p_S)x_2[y_0 + (1-p_I)(y_1+y_2)]}{n^*} - ry_2 - \mu y_2\right) \\
&= -\frac{\mu}{x_0^*}(x_0 - x_0^*)^2 - \frac{\alpha}{x_0^* n^*}[y_0 + (1-p_I)(y_1+y_2)](x_0 - x_0^*)^2 \\
&\quad + (r+\mu)\left(\frac{\alpha x_0^*}{r+\mu} \times \frac{y_0 + (1-p_I)(y_1+y_2)}{n^*} - y_0\right) \\
&\quad - \frac{\mu}{x_1^*}(1-p_I)(x_1 - x_1^*)^2 - \frac{\alpha}{x_1^* n^*}(1-p_I)[y_0 + (1-p_I)(y_1+y_2)](x_1 - x_1^*)^2
\end{aligned}$$

$$
\begin{aligned}
&+(r+\mu)(1-p_I)\left(\frac{\alpha x_1^*}{r+\mu}\times\frac{y_0+(1-p_I)(y_1+y_2)}{n^*}-y_1\right)\\
&-\frac{\mu}{x_2^*}(1-p_I)(x_2-x_2^*)^2-\frac{\alpha}{x_2^*n^*}(1-p_S)(1-p_I)[y_0+(1-p_I)(y_1+y_2)](x_2-x_2^*)^2\\
&+(r+\mu)(1-p_I)\left(\frac{\alpha(1-p_S)x_2^*}{r+\mu}\times\frac{y_0+(1-p_I)(y_1+y_2)}{n^*}-y_2\right).
\end{aligned}
\tag{B.1}
$$

In Equation (B.1), we used $x_0^* = \varepsilon_0\Lambda/\mu$, $x_1^* = \varepsilon_1\Lambda/\mu$, $x_2^* = \varepsilon_2\Lambda/\mu$.

We can further deflate Equation (B.1),

$$
\begin{aligned}
&\dot{\mathscr{L}}(\mathbf{\Phi}_1)\\
&-\frac{\mu}{x_1^*}(1-p_I)(x_1-x_1^*)^2-\frac{\alpha}{x_1^*n^*}(1-p_I)[y_0+(1-p_I)(y_1+y_2)](x_1-x_1^*)^2\\
&-\frac{\mu}{x_2^*}(1-p_I)(x_2-x_2^*)^2-\frac{\alpha}{x_2^*n^*}(1-p_S)(1-p_I)[y_0+(1-p_I)(y_1+y_2)](x_2-x_2^*)^2\\
&+(r+\mu)[y_0+(1-p_I)(y_1+y_2)]\left\{\frac{\alpha}{r+\mu}[\varepsilon_0+(1-p_I)\varepsilon_1+(1-p_S)(1-p_I)\varepsilon_2]-1\right\}\\
&=-\frac{\mu}{x_0^*}(x_0-x_0^*)^2-\frac{\alpha}{x_0^*n^*}[y_0+(1-p_I)(y_1+y_2)](x_0-x_0^*)^2\\
&-\frac{\mu}{x_1^*}(1-p_I)(x_1-x_1^*)^2-\frac{\alpha}{x_1^*n^*}(1-p_I)[y_0+(1-p_I)(y_1+y_2)](x_1-x_1^*)^2\\
&-\frac{\mu}{x_2^*}(1-p_I)(x_2-x_2^*)^2-\frac{\alpha}{x_2^*n^*}(1-p_S)(1-p_I)[y_0+(1-p_I)(y_1+y_2)](x_2-x_2^*)^2\\
&+(r+\mu)[y_0+(1-p_I)(y_1+y_2)](\mathscr{R}_0-1)\le 0,
\end{aligned}
\tag{B.2}
$$

which completes the proof.

C. The Existence and Uniqueness of Ψ^{**} When $\mathscr{R}_0 > 1$

Using the equations $\dot{y}_0 = 0$, $\dot{y}_1 = 0$, $\dot{y}_2 = 0$ in $\dot{\Psi} = 0$ to obtain x_i^{**} as a function of y_i^{**}, $i = 0, 1, 2$. Then, substituting the results into the equations $\dot{x}_0 = 0$, $\dot{x}_1 = 0$, $\dot{x}_2 = 0$,

$$
\begin{cases}
0 = \varepsilon_0\Lambda-(r+\mu)y_0^{**}-\dfrac{\mu n^*(r+\mu)y_0^{**}}{\alpha[y_0^{**}+(1-p_I)(y_1^{**}+y_2^{**})]},\\
0 = \varepsilon_1\Lambda-(r+\mu)y_1^{**}-\dfrac{\mu n^*(r+\mu)y_1^{**}}{\alpha[y_0^{**}+(1-p_I)(y_1^{**}+y_2^{**})]},\\
0 = \varepsilon_2\Lambda-(r+\mu)y_2^{**}-\dfrac{\mu n^*(r+\mu)y_2^{**}}{\alpha(1-p_S)[y_0^{**}+(1-p_I)(y_1^{**}+y_2^{**})]}.
\end{cases}
\tag{C.1}
$$

In Equation (C.1), the authors multiply the first equation by $\alpha/(r+\mu)$, the second equation by $\alpha(1-p_I)/(r+\mu)$, and the third equation by $\alpha(1-p_S)(1-p_I)/(r+\mu)$:

$$\begin{cases} 0 = \dfrac{\alpha}{r+\mu}\varepsilon_0\Lambda - \alpha y_0^{**} - \dfrac{\mu n^* y_0^{**}}{y_0^{**} + (1-p_I)(y_1^{**} + y_2^{**})}, \\ 0 = \dfrac{\alpha}{r+\mu}(1-p_I)\varepsilon_1\Lambda - \alpha(1-p_I)y_1^{**} - \dfrac{\mu n^*(1-p_I)y_1^{**}}{y_0^{**} + (1-p_I)(y_1^{**} + y_2^{**})}, \\ 0 = \dfrac{\alpha}{r+\mu}(1-p_S)(1-p_I)\varepsilon_2\Lambda - \alpha(1-p_S)(1-p_I)y_2^{**} - \dfrac{\mu n^*(1-p_I)y_2^{**}}{y_0^{**} + (1-p_I)(y_1^{**} + y_2^{**})}. \end{cases} \tag{C.2}$$

Summing up the three equations in Equation (C.2) and using $n^* = \Lambda/\mu$ (see Equation (4)), the authors have

$$\mathscr{R}_0 - \alpha[y_0^{**} + (1-p_I)y_1^{**} + (1-p_S)(1-p_I)y_2^{**}] - 1 = 0. \tag{C.3}$$

Therefore, to ensure $y_0^{**} + (1-p_I)y_1^{**} + (1-p_S)(1-p_I)y_2^{**} > 0$, which is a necessary condition for $y_0^{**} > 0$, $y_1^{**} > 0$, $y_2^{**} > 0$, the authors have $\mathscr{R}_0 > 1$. However, the authors have not yet proved that $\mathscr{R}_0 > 1$ is a sufficient condition for $y_0^{**} > 0$, $y_1^{**} > 0$, $y_2^{**} > 0$.

According to Equation (C.2), the authors can ensure $y_0^{**} > 0$, $y_1^{**} > 0$, $y_2^{**} > 0$ if the authors can confirm $y_0^{**} + (1-p_I)(y_1^{**} + y_2^{**}) > 0$. We will try to illustrate the opposite case, $y_0^{**} + (1-p_I)(y_1^{**} + y_2^{**}) < 0$, cannot happen. Let us further write Equation (C.2) as

$$\begin{cases} y_0^{**} = \dfrac{\alpha/r + \mu\varepsilon_0\Lambda}{\alpha + \mu n^*/y_0^{**} + (1-p_I)(y_1^{**} + y_2^{**})}, \\ y_1^{**} = \dfrac{\alpha/r + \mu\varepsilon_1\Lambda}{\alpha + \mu n^*/y_0^{**} + (1-p_I)(y_1^{**} + y_2^{**})}, \\ y_2^{**} = \dfrac{\alpha/r + \mu(1-p_S)\varepsilon_2\Lambda}{\alpha(1-p_S) + \mu n^*/y_0^{**} + (1-p_I)(y_1^{**} + y_2^{**})}. \end{cases} \tag{C.4}$$

Then, it can be judged that y_0^{**} and y_1^{**} have the same sign because the denominators are equal and the numerators are both positive. The case $y_0^{**} < 0$, $y_1^{**} < 0$ is possible only if their denominators $\alpha + \mu n^*/[y_0^{**} + (1-p_I)(y_1^{**} + y_2^{**})] < 0$. In this case, the authors have $\alpha(1-p_S) + \mu n^*/[y_0^{**} + (1-p_I)(y_1^{**} + y_2^{**})] < \alpha + \mu n^*/[y_0^{**} + (1-p_I)(y_1^{**} + y_2^{**})] < 0$, which means $y_2^{**} < 0$ as well. Then, the authors have $y_0^{**} + (1-p_I)y_1^{**} + (1-p_S)(1-p_I)y_2^{**} < 0$ because $y_0^{**} < 0$, $y_1^{**} < 0$, $y_2^{**} < 0$, which is inconsistent with our previous conclusion. Therefore, $y_0^{**} > 0$, $y_1^{**} > 0$ must hold.

The remaining question is the sign of y_2^{**}. According to the second equation in Equation (1), the authors have

$$y_0^{**} = \frac{\alpha}{r+\mu}x_0^{**}\frac{[y_0^{**} + (1-p_I)(y_1^{**} + y_2^{**})]}{n^*}. \tag{C.5}$$

Since the authors have $y_0^{**} > 0$, the authors know $x_0^{**}[y_0^{**} + (1-p_I)(y_1^{**} + y_2^{**})] > 0$ as well. The sign of x_0^{**} can be easily judged: if $x_0 = 0$, then $\dot{x}_0 = \varepsilon_0\Lambda > 0$ so that $x_0 < 0$ never happens if the system starts evolving from a meaningful initial state where $x_0 > 0$. Therefore, $x_0^{**} > 0$ and $y_0^{**} + (1-p_I)(y_1^{**} + y_2^{**}) > 0$ must hold as well. Then, $y_2^{**} > 0$ is ensured by the third equation in Equation (C.4).

Therefore, $\mathscr{R}_0 > 1$ is a sufficient and necessary condition for $y_0^{**} > 0$, $y_1^{**} > 0$, $y_2^{**} > 0$.

To check if the solution of y_0^{**}, y_1^{**}, and y_2^{**} really exists, the authors can study the existence of $y_0^{**} + (1-p_I)(y_1^{**} + y_2^{**})$. Then, the solution of y_0^{**}, y_1^{**}, and y_2^{**} can be naturally obtained by Equation (C.4). For convenience, the authors denote $Y = y_0^{**} + (1-p_I)(y_1^{**} + y_2^{**})$. Multiplying the three equations of y_0^{**}, y_1^{**}, y_2^{**} in Equation (C.4) by 1, $1-p_I$, $1-p_I$, and adding them together, the authors get

$$Y = \frac{\alpha/r + \mu\varepsilon_0\Lambda}{\alpha + \mu n^*/Y} + (1-p_I)\frac{\alpha/r + \mu\varepsilon_1\Lambda}{\alpha + \mu n^*/Y} + (1-p_I)\frac{\alpha/r + \mu(1-p_S)\varepsilon_2\Lambda}{\alpha(1-p_S) + \mu n^*/Y}, \tag{C.6}$$

which can be simplified as follows when $Y \neq 0$.

$$aY^2 + bY + c = 0, \tag{C.7}$$

where

$$\begin{cases} a = \dfrac{\alpha}{\mu n^*}(1 - p_S), \\ b = 1 - p_S + 1 - \mathscr{R}_0 + \dfrac{\alpha}{r + \mu} p_S(\varepsilon_0 + (1 - p_I)\varepsilon_1), \\ c = \dfrac{\mu n^*}{\alpha}(1 - \mathscr{R}_0). \end{cases} \quad \text{(C.8)}$$

We can see that $a > 0$ always holds. The signs of b and c, however, depend on $\mathscr{R}_0$. Then, the simple use of Vieta's theorem can judge the existence of Y. When $\mathscr{R}_0 < 1$, the authors have $c/a > 0$ and $-b/a < 0$; therefore, both roots are negative. When $\mathscr{R}_0 > 1$, the authors have $c/a < 0$; therefore, one root is positive and the other is negative. The positive root is the unique solution of Y and $y_0^{**} + (1 - p_I)(y_1^{**} + y_2^{**})$. Then, Equation (C.4) can provide the unique solution of y_0^{**}, y_1^{**}, and y_2^{**} (note that the negative root of Y cannot lead to positive y_0^{**}, y_1^{**}, and y_2^{**} because the authors have previously shown $y_0^{**} > 0$, $y_1^{**} > 0$, and $y_2^{**} > 0$ if $\mathscr{R}_0 > 1$).

Data Availability

Data sharing is not applicable to this article as no datasets were generated or analyzed during the current study.

Conflicts of Interest

The authors declare that they have no conflicts of interest.

Acknowledgments

The publication of this article was funded in part by the George Mason University Libraries Open Access Publishing Fund.

References

[1] L. Peeples, "Face masks for COVID pass their largest test yet," *Nature (London)*, 2021.

[2] W. O. Kermack and A. G. McKendrick, "A contribution to the mathematical theory of epidemics," *Proceedings of the Royal Society of London*, vol. 115, no. 772, pp. 700–721, 1927.

[3] N. S. Barlow and S. J. Weinstein, "Accurate closed-form solution of the SIR epidemic model," *Physica D: Nonlinear Phenomena*, vol. 408, Article ID 132540, 2020.

[4] S. J. Weinstein, M. S. Holland, K. E. Rogers, and N. S. Barlow, "Analytic solution of the SEIR epidemic model via asymptotic approximant," *Physica D: Nonlinear Phenomena*, vol. 411, Article ID 132633, 2020.

[5] C. Wang and C. Huang, "An epidemic model with the closed management in Chinese universities for COVID-19 prevention," in *Journal of Physics: Conference Series*vol. 1707, IOP Publishing, Article ID 012027, 2020.

[6] X. Wang, H. Peng, B. Shi, D. Jiang, S. Zhang, and B. Chen, "Optimal vaccination strategy of a constrained time-varying SEIR epidemic model," *Communications in Nonlinear Science and Numerical Simulation*, vol. 67, pp. 37–48, 2019.

[7] F. Fu, D. I. Rosenbloom, L. Wang, and M. A. Nowak, "Imitation dynamics of vaccination behaviour on social networks," *Proceedings of the Royal Society B: Biological Sciences*, vol. 278, pp. 42–49, 2011.

[8] X. Wang, D. Jia, S. Gao, C. Xia, X. Li, and Z. Wang, "Vaccination behavior by coupling the epidemic spreading with the human decision under the game theory," *Applied Mathematics and Computation*, vol. 380, Article ID 125232, 2020.

[9] M. Alam, K. Kuga, and J. Tanimoto, "Three-strategy and four-strategy model of vaccination game introducing an intermediate protecting measure," *Applied Mathematics and Computation*, vol. 346, pp. 408–422, 2019.

[10] K. Kuga and J. Tanimoto, "Which is more effective for suppressing an infectious disease: imperfect vaccination or defense against contagion?" *Journal of Statistical Mechanics: Theory and Experiment*, vol. 2018, Article ID 023407, 2018.

[11] M. Alam, M. Tanaka, and J. Tanimoto, "A game theoretic approach to discuss the positive secondary effect of vaccination scheme in an infinite and well-mixed population," *Chaos, Solitons & Fractals*, vol. 125, pp. 201–213, 2019.

[12] L. Zhao, Q. Wang, J. Cheng, Y. Chen, J. Wang, and W. Huang, "Rumor spreading model with consideration of forgetting mechanism: a case of online blogging livejournal," *Physica A: Statistical Mechanics and Its Applications*, vol. 390, no. 13, pp. 2619–2625, 2011.

[13] L. Zhao, W. Xie, H. O. Gao, X. Qiu, X. Wang, and S. Zhang, "A rumor spreading model with variable forgetting rate," *Physica A: Statistical Mechanics and Its Applications*, vol. 392, no. 23, pp. 6146–6154, 2013.

[14] C. Wang, "Dynamics of conflicting opinions considering rationality," *Physica A: Statistical Mechanics and Its Applications*, vol. 560, Article ID 125160, 2020.

[15] C. Wang, Z. Wang, and Q. Pan, "Injurious information propagation and its global stability considering activity and normalized recovering rate," *PLoS One*, vol. 16, no. 10, Article ID e0258859, 2021.

[16] C. Vargas-De-León, "On the global stability of SIS, SIR and SIRS epidemic models with standard incidence," *Chaos, Solitons & Fractals*, vol. 44, no. 12, pp. 1106–1110, 2011.

[17] J. Li, Y. Xiao, F. Zhang, and Y. Yang, "An algebraic approach to proving the global stability of a class of epidemic models," *Nonlinear Analysis: Real World Applications*, vol. 13, no. 5, pp. 2006–2016, 2012.

[18] S. Side, W. Sanusi, M. K. Aidid, and S. Sidjara, "Global stability of SIR and SEIR model for tuberculosis disease transmission with lyapunov function method," *Asian Journal of Applied Sciences*, vol. 9, no. 3, pp. 87–96, 2016.

[19] H. Guo, M. Y. Li, and Z. Shuai, "Global stability of the endemic equilibrium of multigroup SIR epidemic models," *Canadian Applied Mathematics Quarterly*, vol. 14, no. 3, pp. 259–284, 2006.

[20] R. Sun, "Global stability of the endemic equilibrium of multigroup SIR models with nonlinear incidence," *Computers & Mathematics with Applications*, vol. 60, no. 8, pp. 2286–2291, 2010.

[21] Y. Muroya, Y. Enatsu, and T. Kuniya, "Global stability for a multi-group SIRS epidemic model with varying population sizes," *Nonlinear Analysis: Real World Applications*, vol. 14, no. 3, pp. 1693–1704, 2013.

[22] L. Cheng, L. Yin, J. Wang et al., "Behavioral decision-making in power demand-side response management: a multi-population evolutionary game dynamics perspective,"

International Journal of Electrical Power & Energy Systems, vol. 129, Article ID 106743, 2021.

[23] L. Cheng, Y. Chen, and G. Liu, "2PnS-EG: a general two-population *n*-strategy evolutionary game for strategic long-term bidding in a deregulated market under different market clearing mechanisms," *International Journal of Electrical Power & Energy Systems*, vol. 142, Article ID 108182, 2022.

[24] W. Li, J. Zhou, and J.-A. Lu, "The effect of behavior of wearing masks on epidemic dynamics," *Nonlinear Dynamics*, vol. 101, no. 3, pp. 1995–2001, 2020.

[25] J. A. Gondim, "Preventing epidemics by wearing masks: an application to COVID-19," *Chaos, Solitons & Fractals*, vol. 143, Article ID 110599, 2021.

[26] P. Auger and A. Moussaoui, "On the threshold of release of confinement in an epidemic SEIR model taking into account the protective effect of mask," *Bulletin of Mathematical Biology*, vol. 83, no. 4, pp. 1–18, 2021.

[27] N. O. Lasisi and K. A. Adeyemo, "Modeling the effect of distancing and wearing of face masks on transmission of Covid-19 infection dynamics," *Journal of Complexity in Health Sciences*, vol. 4, no. 1, pp. 10–20, 2021.

[28] L. Han, Q. Pan, B. Kang, and M. He, "Effects of masks on the transmission of infectious diseases," *Advances in Difference Equations*, vol. 2021, no. 1, 17 pages, 2021.

[29] E. P. Scott, *The Model Thinker: What You Need to Know to Make Data Work for You*, Basic Books, New York, NY, USA, 2018.

[30] S. G. Sociophysics, *A Physicist's Modeling of Psycho-Political Phenomena*, Springer, Berlin, Germany, 2016.

[31] P. Van den Driessche and J. Watmough, "Reproduction numbers and sub-threshold endemic equilibria for compartmental models of disease transmission," *Mathematical Biosciences*, vol. 180, no. 1-2, pp. 29–48, 2002.

[32] J. P. La Salle, *The Stability of Dynamical Systems*, SIAM, Thailand, 1976.

[33] M. A. Boraey, "An analytical model for the effective filtration efficiency of single and multiple face masks considering leakage," *Chaos, Solitons & Fractals*, vol. 152, Article ID 111466, 2021.